CHEMISTRY OF MATERIALS
Article

Chem. Mater. **2010,** *22,* 155–160 155
DOI:10.1021/cm902527n

Bottom-up Fabrication of Metal/Metal Nanocomposites from Nanoparticles of Immiscible Metals

Norman A. Luechinger, Robert N. Grass, Evagelos K. Athanassiou, and Wendelin J. Stark*

Institute for Chemical and Bioengineering Department of Chemistry and Applied Biosciences ETH Zurich, CH-8093 Zurich, Switzerland

Received August 17, 2009. Revised Manuscript Received November 18, 2009

The combination of immiscible metals has traditionally escaped preparation as such metal's largely different surface energies lead to nonwetting and separation of the two metals during synthesis. The simultaneous preparation of two metals as nanoparticles in a gas phase process can result in the formation of random agglomerates if rapidly cooled. Compaction and subsequent sintering then allows combining otherwise immiscible metals in a bottom-up approach to form metal/metal nanocomposites. In this work, bismuth and cobalt were chosen as model materials which cannot be alloyed by traditional metallurgy due to their large difference in physical properties such as hardness and melting point. Combining bismuth with cobalt (continuous phase) at the nanometer scale resulted in a metal/metal nanocomposite. This class of materials is formally an extension of the current oxide/metal nanocomposites which we conceptually demonstrated through the combination of two distinctly different properties of the composite's base metals: The bismuth/cobalt nanocomposite displayed a low friction value of around 0.2 (a property of soft bismuth) while maintaining a high hardness (a property of nanocrystalline cobalt). These previously difficult to access properties are attractive for the development of lead-free bearings in energy efficient engines.

Introduction

Bulk nanocomposite materials are among the most rapidly moving fields in materials science since they can be designed from nontraditional combinations of constituents. Metal/metal nanocomposites result from nonmiscible metals and give access to fascinating alternatives to traditional metal alloys with superior mechanical,[1−3] magnetic,[4−6] or tribological properties.[1,7,8] The beneficial effects are the result of combining metals of completely different physical properties at the nanometer scale. Generally, such metal mixtures have been difficult to prepare when using traditional metallurgy which has motivated the development of mechanical alloying, severe plastic deformation, or rapid solidification (see Supporting Information Table ST1 for an overview).[1−6,8−13] These top-down approaches have yielded fascinating improvements in metallurgy, but they require vast amounts of energy and long processing time.

An elegant bottom-up technique for intermetallic and alloy nanocomposites has been proposed based on the preparation of the corresponding composite nanoparticles.[14,15] In contrast to the use of miscible components, Grass et al. recently demonstrated the homogeneous mixing of over 20 vol % of a hard ceramic (cerium oxide, a refractory ceramic) into a soft metal (bismuth) at the 50 nm scale—this extension of classical oxide reinforcement to 1 order of magnitude higher loadings was the result of mixing the constituents bottom-up, as nanoparticles. The only way to avoid demixing was to manufacture the constituents at the same time and irreversibly agglomerate them right during powder collection. Using such bottom-up preparations, we most recently reported on the tripled Vickers hardness both in nanocrystalline cobalt[16] and superalloy (Ni/Mo)[17] prepared from the corresponding metal or alloy nanoparticles. Bottom-up

*Corresponding author. Fax: +41 44 633 1083. E-mail: wstark@ethz.ch.

(1) Liu, X.; Zeng, M. Q.; Ma, Y.; Zhu, M. *Wear* **2008**, *265*, 1857.
(2) Sauvage, X.; Jessner, P.; Vurpillot, F.; Pippan, R. *Scr. Mater.* **2008**, *58*, 1125.
(3) Noskova, N. I.; Vil'danova, N. F.; Filippov, Y. I.; Churbaev, R. V.; Pereturina, I. A.; Korshunov, L. G.; Korznikov, A. V. *Phys. Met. Metall.* **2006**, *102*, 646.
(4) Bose, S.; Bhattacharya, V.; Chattopadhyay, K.; Ayyub, P. *Acta Mater.* **2008**, *56*, 4522.
(5) Saha, S.; Kulovits, A.; Soffa, W. A.; Barnard, J. A. *J. Appl. Phys.* **2005**, 97.
(6) Drbohlav, O.; Yavari, A. R. *Acta Metall. Mater.* **1995**, *43*, 1799.
(7) Bhattacharya, V.; Chattopadhyay, K. *Acta Mater.* **2004**, *52*, 2293.
(8) Zhu, M.; Gao, Y.; Chung, C. Y.; Che, Z. X.; Luo, K. C.; Li, B. L. *Wear* **2000**, *242*, 47.
(9) Bhattacharya, V.; Yamasue, E.; Ishihara, K. N.; Chattopadhyay, K. *Acta Mater.* **2005**, *53*, 4593.
(10) Chattopadhyay, K.; Goswami, R. *Prog. Mater. Sci.* **1997**, *42*, 287.
(11) Golubkova, G. V.; Lomovsky, O. I.; Kwon, Y. S.; Vlasov, A. A.; Chuvilin, A. L. *J. Alloys Compd.* **2003**, *351*, 101.
(12) Sabirov, I.; Pippan, R. *Scr. Mater.* **2005**, *52*, 1293.
(13) Yavari, A. R.; Desre, P. J.; Benameur, T. *Phys. Rev. Lett.* **1992**, *68*, 2235.
(14) Cable, R. E.; Schaak, R. E. *Chem. Mater.* **2007**, *19*, 4098.
(15) Haber, J. A.; Gunda, N. V.; Balbach, J. J.; Conradi, M. S.; Buhro, W. E. *Chem. Mater.* **2000**, *12*, 973.
(16) Grass, R. N.; Dietiker, M.; Solenthaler, C.; Spolenak, R.; Stark, W. J. *Nanotechnology* **2007**, 18.
(17) Athanassiou, E. K.; Grass, R. N.; Osterwalder, N.; Stark, W. J. *Chem. Mater.* **2007**, *19*, 4847.

Published on Web 12/07/2009

fabrication was first reported by Odeh et al. for micrometer-sized metal mixtures of cobalt and bismuth obtained from wet phase precipitation.[18]

Here, we demonstrate the preparation of bulk metal/metal nanocomposites from nonmiscible metals by using reducing flame spray synthesis[19,20] for the simultaneous fabrication of the individual metal constituents. As a model system, we also chose bismuth and cobalt as they represent two extremely different metals: Bismuth is one of the softest metals with a melting point of around 270 °C. Cobalt is a key part in hard metals and refractory alloys and melts at 1495 °C. Combining the hardness of cobalt and the softness of bismuth afforded a metal/metal nanocomposite with excellent lubrication properties. A potential application of such composites is in the replacement of lead or carbon-based bearings in engines where reduced wear at high lubrication are crucial to achieve high mechanical efficiency. This is of particular importance in combustion engines where over 30% of the fuel losses are attributed to friction. Bulk bismuth/cobalt nanocomposites may further be suggested for specific magnetic applications since Bi/Co thin films have been reported to exhibit promising magnetic properties.[21−23]

Experimental Section

Chemicals and Reagents. Bismuth 2-ethylhexanoate was purchased from ABCR (25% Bi content). Cobalt 2-ethylhexanoate was prepared from 2-ethylhexanoic acid (Fluka, purum) and cobalt acetate tetra hydrate (ABCR, 98% purity) by distilling off acetic acid at 150 °C for 2 h. For the different bismuth and cobalt contents of the nanocomposites, the two precursors were mixed in corresponding ratios. Each solution was diluted 2:1 (weight/weight) with tetrahydrofuran (Fluka, tech.) and filtered (Satorius, fluted filter type 288) prior to use.

Metal Nanopowder Synthesis. The carboxylate-based precursors[24] were fed (6 mL min^{-1}, HNP Mikrosysteme, micro annular gear pump mzr-2900) to a spray nozzle which was placed in a glovebox.[25] The enclosed atmosphere consisted of nitrogen (PanGas, 5.0) which was recirculated by a vacuum pump (Busch, Seco SV1040CV) at about 20 m^3 h^{-1}.[20,25] The precursors were dispersed by oxygen (5 L min^{-1}, PanGas tech.) and ignited by a premixed methane−oxygen flame (CH_4 1.2 L min^{-1}, O_2 2.2 L min^{-1}, PanGas tech.).[26] CO_2 and H_2O were continuously removed from the recycle stream using two adsorption columns, packed with zeolite 4A and 13X (Zeochem), respectively. To avoid the accumulation of CO, NO and other impurities in the glovebox atmosphere a purge gas stream continuously passed through the box. A sinter metal tube (GKN Sintermetalle, 25 mm inner diameter) surrounding the flame allowed radial inflow of CO_2 (PanGas, 99.995%) at a flow rate of 25 L min^{-1}. An oxygen concentration of below 100 ppm (volume/volume) was maintained during all synthesis experiments in the glovebox. The produced particles were separated from the off-gas using glass fiber filters (Schleicher & Schuell, GF6).

Before further treatment, the metal nanopowders were passivated by a protecting thin oxide layer in order to avoid pyrophoricity when brought into contact with air. More specifically, 300 mg of metal powder was enclosed in a pill glass of 30 mL and taken out of the glovebox. A volume of 5 mL air was gently injected with a syringe. This step was repeated twice while waiting 1 min in between injection steps. Finally, the cap of the bottle was removed for 30 min in order to fully complete the passivation reaction. The passivated powders could then be handled at ambient conditions without spontaneous ignition. The amount of oxygen uptake was around 4 wt % (Supporting Information Figure S1) as measured by thermogravimetry (see below).

Nanocomposite Fabrication. Bulk composite samples were prepared by pressing 300 mg of passivated metal nanopowder into pills with a diameter of 1.25 cm, using a uniaxial press at 400 MPa during 5 min. Sintering of the metal pills was performed in a tube oven (Carbolite, 12/38/400) with a constant flow of hydrargon 7 (7 vol % H_2 in argon, PanGas). The heating rate was 10 °C min^{-1}, and a dwell time of 30 min was applied. The cooling temperature profile was nonlinear (Supporting Information Figure S3).

Powder Characterization Methods. The weight gain (uptake of oxygen) during the passivation procedure was determined gravimetrically. The as-produced powders were analyzed by X-ray diffraction (Siemens powder X-ray diffractometer with a Ni-filtered Cu Kα radiation, step size 0.03°). The carbon content of the sintered samples was measured by microanalysis (LECO, CHN-900). The specific surface area was obtained by nitrogen adsorption (BET, Tristar Micromeritics Instruments). For scanning transmission electron microscopy (STEM), the powders were suspended in ethanol and deposited onto a perforated carbon foil supported on a copper grid. The investigations were performed on a Tecnai F30 microscope (FEI Eindhoven; field emission cathode, operated at 300 kV). STEM images were obtained with a high-angle annular dark field (HAADF) detector. An energy filter (Gatan imaging filter, GIF) installed below the Tecnai 30 FEG allowed recording electron energy loss spectra (EELS) and element specific images (elemental maps) by means of the electron spectroscopic imaging (ESI) technique.

Bismuth contents of the different powder samples were verified by atomic absorption spectroscopy (AAS, Perkin-Elmer Analyst 200, 1.8 nm slit width, air/acetylene flame). Prior to analysis, powders were dissolved in nitric acid and diluted to about 5 ppm Bi.

Metal/Metal Nanocomposite Characterization and Tribological Tests. The as-pressed and later sintered pills were analyzed separately by scanning electron microscopy (LEO 1530 Gemini, accelerating voltage 5 kV). The sintered pills were embedded in Bakelite for 3 min at 180 °C and a pressure of 25 MPa. Vickers microhardness HV0.1 (MTX-α, Wolpert) was measured after polishing the embedded pills with 500-, 2400-, and 4000-grit grinding paper and finally a 50 nm-diamond suspension. Polished pills were analyzed by X-ray diffraction (Panalytical X'Pert PRO-MPD, step size 0.05°). The initial-stage dynamic coefficient of friction of the polished surfaces was tested at dry conditions against a 100Cr6 steel ball (Hydrel, 6 mm diameter,

(18) Odeh, I. M.; Mahmoud, S.; Vassilev, G. P. *Int. J. Mater. Res.* **2007**, *98*, 884.
(19) Athanassiou, E. K.; Grass, R. N.; Stark, W. J. *Nanotechnology* **2006**, *17*, 1668.
(20) Grass, R. N.; Stark, W. J. *J. Mater. Chem.* **2006**, *16*, 1825.
(21) Hsu, J. H.; Xue, Z. L.; Huang, T. C.; Wei, Z. H.; Lai, M. F. *J. Magn. Magn. Mater.* **2007**, *310*, 2239.
(22) Li, G. R.; Ke, Q. F.; Liu, G. K.; Liu, P.; Tong, Y. X. *Mater. Lett.* **2007**, *61*, 884.
(23) Yang, G. H.; Chen, J. B.; Zhao, B.; Pan, F. *J. Alloy. Compd.* **2004**, *365*, 43.
(24) Stark, W. J.; Madler, L.; Maciejewski, M.; Pratsinis, S. E.; Baiker, A. *Chem. Commun.* **2003**, 588.
(25) Grass, R. N.; Stark, W. J. *J. Nanopart. Res.* **2006**, *8*, 729.
(26) Madler, L.; Stark, W. J.; Pratsinis, S. E. *J. Mater. Res.* **2002**, *17*, 1356.

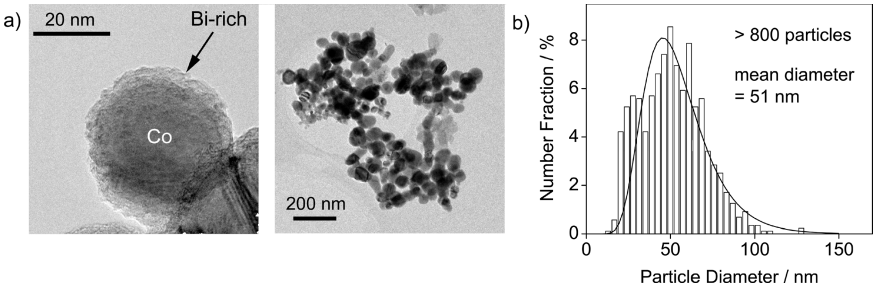

Figure 1. Metal nanoparticles consisting of 25 wt % bismuth and 75 wt % cobalt (electron micrograph, a). Individual nanoparticles consist of a cobalt core and a bismuth rich shell as further confirmed by energy dispersive X-ray spectroscopy (EDXS). (b) Primary particle size distributions obtained by optically determining the size of at least 800 individual particles on electron micrographs.

HRC 58−66, Ramax = 15 nm, DIN 5401) on a ball-on-disk setup (CSM Tribometer) at relative humidities between 30 and 40% and 25 °C. Before friction testing, steel balls were ultrasonicated in ethanol for 5 min. The relative sliding speed between the friction partners was always kept 2 cm s^{-1} at an applied load of 2 N. In each friction test, the mean coefficient of friction was determined by averaging the data over the second half of 100 revolutions (laps) in order to exclude initial friction fluctuations.

Results and Discussion

The basic ingredient for the preparation of a bismuth/cobalt metal/metal nanocomposite was synthesized by reducing flame synthesis. This process combusts metal-containing fuels in flames of about 1000 °C under reducing conditions and yields metal nanoparticles of 10−50 nm size.[20,25] A systematic investigation of the influence of composition (Bi/Co ratio) on the final properties of the metal/metal nanocomposite (friction coefficient; hardness) was based on the preparation of a series of bismuth/cobalt nanopowders ranging from pure cobalt to samples with 25 wt % bismuth (see Supporting Information Table ST2). A detailed description of the preparation process used here, reducing flame synthesis, is given by Grass et al. who first demonstrated the successful preparation of metallic nanoparticles by flame synthesis using an enclosed reaction chamber with a reducing atmosphere.[27,28] The resulting metal nanoparticles after synthesis consisted of a lightweight, black powder consisting of 20−80 nm size metal particles (Figure 1). Electron microscopy investigations and element sensitive mapping (Supporting Information Figure S2) confirmed the presence of a cobalt metal rich core and a bismuth rich shell layer. Flame-synthesized composite oxide nanoparticles had already been reported earlier with a similar structure.[29,30]

The particles displayed a log-normal size distribution (Figure 1b) in agreement with the theoretical understanding of the particle formation process.[31,32] van der Waals forces (unspecific attraction of particles) group the individual primary particles in soft agglomerates during collection (Figure 1a). The visually determined particle size (average particle size 51 nm) stays in agreement with surface-equivalent primary particle sizes (specific surface area: 16 m^2 g^{-1}; corresponding surface area equivalent particle size assuming spherical particles: 42 nm) as determined by nitrogen adsorption according to the BET method. Since carbon was often found as an impurity in metal nanoparticles, element microanalysis was used to measure the C content. All samples (Bi/Co compositions) exhibited a carbon content below 1.8 wt % (see Supporting Information Table ST2) and stayed of similar size irrespectible of composition. Rapid sample exposure to air (the synthesis proceeds under a nitrogen atmosphere with 1−3% hydrogen) demonstrated the nanometal's pyrophoricity. In order to avoid ignition of the pyrophoric powder, as-prepared particles were surface-oxidized (formation of a protecting oxide layer on individual nanoparticles) through slowly diffusing air into sample vials (see the Experimental Section and Supporting Information Figure S1 for details) which resulted in an approximate oxygen uptake of 4 wt %. During this passivation step, part of the metallic bismuth was oxidized to Bi_2O_3 due to its proximity to the surface.

The phase composition of the metal nanopowders was investigated by X-ray diffraction (Supporting Information Figure S6). All diffractograms showed characteristic peaks for pure, metallic fcc-cobalt as main constituent of all the materials. For high Bi content (26 Bi), passivated (i.e., surface oxidized) samples showed a broad signal around 30° 2θ which fits the characteristic signals of bismuth oxide Bi_2O_3.

The absence of sharp, distinct bismuth metal signals is again evidence that no separate bismuth metal nanoparticles with a size comparable to cobalt were formed during synthesis.[27] This therefore again corroborates the assumption that bismuth deposited on the surface of previously formed cobalt nanoparticles during synthesis. This also confirms the high uniformity of these samples as later visible during sample compaction (see below, Figure 2).

(27) Grass, R. N.; Albrecht, T. F.; Krumeich, F.; Stark, W. J. *J. Mater. Chem.* **2007**, *17*, 1485.
(28) Grass, R. N.; Athanassiou, E. K.; Stark, W. J. *Angew. Chem.-Int. Edit.* **2007**, *46*, 4909.
(29) Loher, S.; Schneider, O. D.; Maienfisch, T.; Bokorny, S.; Stark, W. J. *Small* **2008**, *4*, 824.
(30) Strobel, R.; Baiker, A.; Pratsinis, S. E. *Adv. Powder Technol.* **2006**, *17*, 457.
(31) Dekkers, P. J.; Friedlander, S. K. *J. Colloid Interface Sci.* **2002**, *248*, 295.
(32) Vemury, S.; Pratsinis, S. E. *J. Aerosol Sci.* **1995**, *26*, 175.

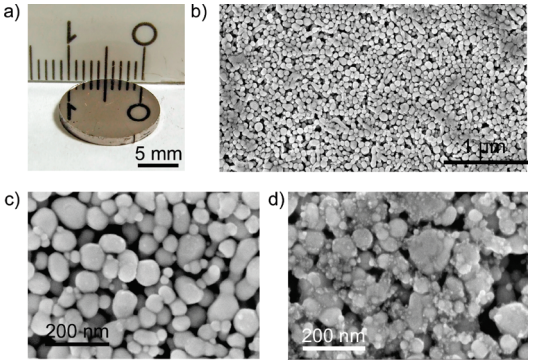

Figure 2. (a) Mechanical compaction of metal/metal nanopowders which resulted in bulk pills exhibiting a mirrorlike surface. (b) Scanning electron microscopy confirmed a high uniformity of the samples exclusively built up from metal nanoparticles. A detailed view illustrates the difference between samples with low (part c sample 0.5 Bi) and high Bi content (part d 48 Bi) where the two immiscible metals provoked an irregular structure.

Bulk nanocomposite materials were obtained from the passivated nanopowders through pressing pills which exhibited a highly metallic appearance (Figure 2a). The morphology of the compacted samples was investigated on the surfaces (part b). The top surface of a pressed pill with small Bi content (0.5 Bi) consisted of densely packed spherical nanoparticles. The absence of large particles confirmed the uniformity of the sample and the well-defined particle size distribution as shown in Figure 1. The porosity of these pills was around 50 vol % as derived from the apparent density (pill weight over mechanically measured pill volume). Figure 2c and d allows a direct comparison of compacted particles of nanopowder 0.5 Bi and 48 Bi. The more irregular structure of 48 Bi can be attributed to the presence of additional bismuth deposits and bismuth oxide impurities.

Pressed pills were sintered in a hydrogen containing atmosphere (7 vol % H_2 in argon) in order to reduce oxide impurities to the corresponding metals ($Bi_2O_3 + 3H_2 \rightarrow 2Bi + 3H_2O$) and strengthen the material by densification. The evolution of sample morphology during sintering was followed by electron micrographs of fracture surfaces taken from pills at a given temperature. Pill fracture surfaces of a series of different nanocomposites are shown for sintering temperatures of 700 °C (Supporting Information Figure S9a−c) and 900 °C (Figure S9d−f). For samples with low Bi content, pills sintered at both sintering temperatures still exhibited significant porosity (Figure S9a and d) in agreement with earlier investigations by Grass et al.[16] on the sintering of pure metal cobalt nanoparticles of similar size. Bulk pills with high homogeneity could be obtained after sintering of nanocomposite 0.5 Bi (Supporting Information Figure S7). This supports the technical feasibility to fabricate bulk parts of the here reported metal/metal nanocomposites.

The crystal phases and the material purity (significant oxide impurities or other byproduct) were investigated by X-ray diffraction of sintered pills (900 °C; Figure 3). In contrast to the exclusive presence of fcc cobalt in as-prepared nanopowders (Supporting Information

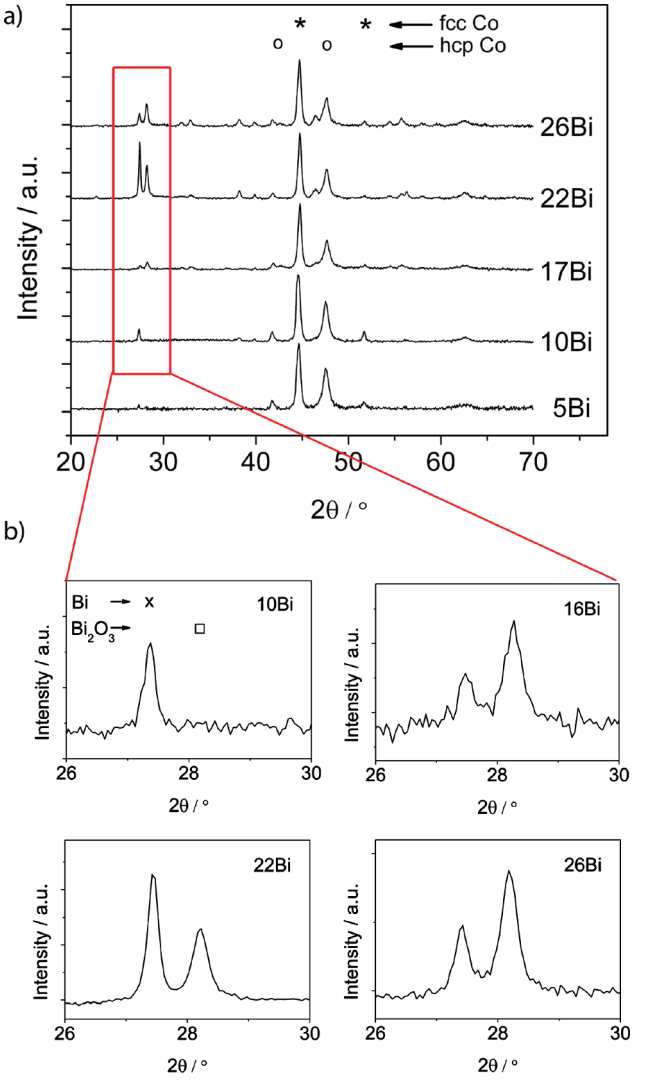

Figure 3. (a) X-ray diffraction patterns of sintered metal/metal composite pills (900 °C) revealing the presence of fcc- and hcp-Co crystal phases (the two major reflexes for each crystal phase are indicated by circles and stars). (b) Detailed view showing characteristic peaks for metallic bismuth (major reflex indicated by a cross) and the oxide (major reflex indicated by a square). At low bismuth loadings (10 Bi), there is no evidence of crystalline bismuth oxide, whereas at higher loadings (17 Bi, 22 Bi, 26 Bi), metallic bismuth is accompanied by Bi_2O_3.

Figure S6), sintered pills contained both fcc and hcp cobalt phases in all samples (part a). At low bismuth loadings (10 Bi), there was no evidence of bismuth oxide impurities (part b), whereas at higher loadings (17 Bi, 22 Bi, 26 Bi), metallic bismuth was accompanied by Bi_2O_3. Significant amounts of bismuth oxide at high bismuth loadings could presumably be related to incomplete reduction of bismuth oxide during sintering as a result of mass transport limitations (limited access of hydrogen to all bismuth oxide in the interior of the sample). However, sample 10 Bi did not show any oxide impurities and presently represents the highest Bi loading still leading to a pure metal/metal nanocomposite. A scanning electron micrograph of nanopowder 10 Bi (Supporting Information Figure S5) showed a very similar morphology to sample 0.5 Bi (Figure 2c) and stays in agreement with above observations.

Scheme 1. Bottom-up Metal/Metal Nanocomposite Fabrication[a]

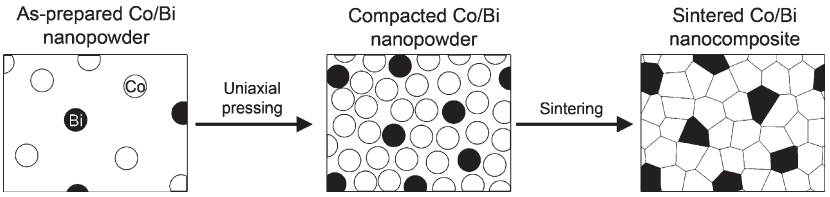

[a] Simultaneously synthesized cobalt and bismuth nanoparticles are already synthesized as a mixture if formed from a homogeneous precursor at similar formation rates. Compaction and subsequent sintering affords densification and strengthening of the resulting metal/metal nanocomposite.

At bismuth contents exceeding 26 wt % (samples 32 Bi and 48 Bi), sintering resulted in squeeze-out of liquid bismuth to the pill surface (Supporting Information Figure S4). Squeeze-out is the direct result of a too high bismuth volume fraction and the force which is exerted to liquid bismuth during neck formation and densification of the cobalt matrix. At such high bismuth loadings, liquid bismuth cannot be entrapped anymore between cobalt grains. Up to a content of 25 wt % bismuth, sintering allows the preparation of homogeneous nanocomposites without showing any macroscopic phase separation. This stays in full agreement with purely geometric considerations. If we consider densely packed spheres, the void volume is around 27% of the total volume. This is close to the here observed limit of Bi uptake (~26%) into the matrix of hard Co particles. The small differences can be attributed to the presence of a particle size distribution rather than perfectly similar sized spheres (Figure 1) and partial sintering of Co which allows Co spheres to move closer to one another. These results demonstrate that two metals with completely different melting points and thermodynamic immiscibility can be combined to stable metal/metal composites. This bottom-up synthesis concept to metal/metal nanocomposites is summarized in Scheme 1.

In order to demonstrate the successful combination of physical properties of two metals, the friction coefficient and the Vickers hardness of the metal/metal nanocomposites prepared here was investigated. Sintered pills were embedded in Bakelite (a polymer resin) and polished to a very low surface roughness in order to ensure well-defined starting conditions for Vickers microhardness testing (HV0.1, MTX-α, Wolpert) and determination of the coefficient of friction. The initial-stage dynamic coefficient of friction of the polished surfaces was tested at dry conditions using a ball-on-disk setup (CSM Tribometer).

The coefficient of friction was tested for all nanocomposites (Figure 4) as a function of bismuth content and continuously decreased for higher bismuth contents. Samples with the maximum Bi content (25 Bi, no squeeze out of excess Bi) reached low friction values around 0.2 which is comparable to graphite, a technically most

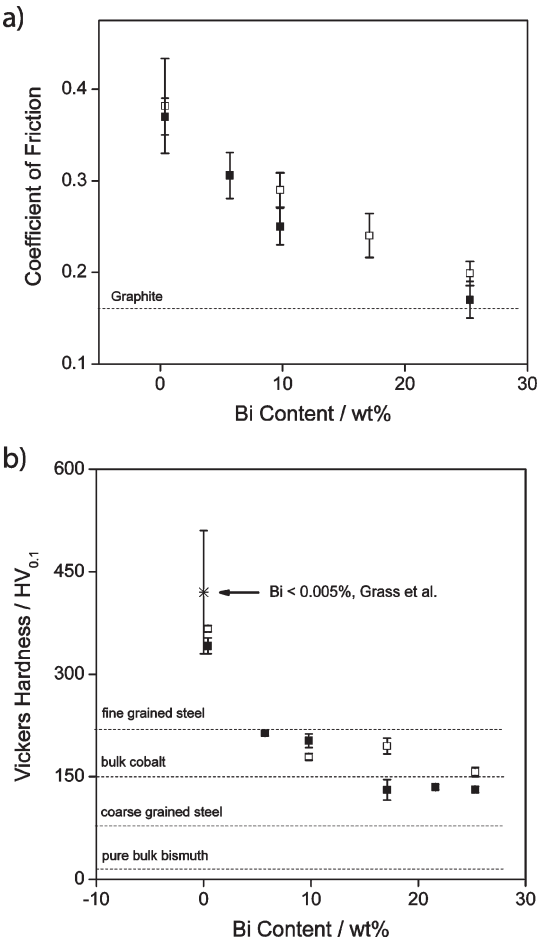

Figure 4. Coefficient of friction (a) and Vickers hardness (b) of polished metal/metal nanocomposite pills sintered at 700 °C (open squares) and 900 °C (filled squares). The range of hardness values at sintering temperatures between 700 and 900 °C reported by Grass et al. is indicated by an asterisk (a different sintering device and sintering profile was used). Dotted lines in part b show reference hardness values for bismuth,[33] coarse and fine grained steels,[34] and bulk cobalt.[35] The dotted line in part a indicates a representative reference value for graphite,[36] one of the materials with the lowest coefficient of friction.

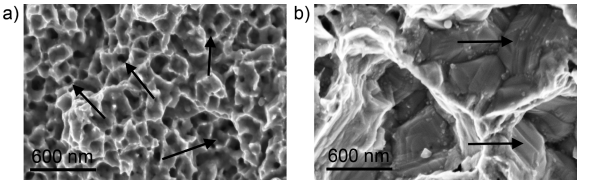

Figure 5. Scanning electron micrographs showing fracture surfaces of sample 0.5 Bi sintered at 700 (a) and 900 °C (b). Nanovoids (arrows in part a) and twin formation (arrows in part b) contribute to the increased hardness values over bulk cobalt.

(33) Rabinowicz. *Friction and Wear of Materials*; Wiley: New York, 1965.
(34) Miyahara, K.; Matsuoka, S.; Hayashi, T. *Metall. Mater. Trans. A* **2001**, *32*, 761.
(35) D., D. J. *Ullmann's Encyclopedia of Industrial Chemistry*; Wiley-VCH: Weinheim, 2003.
(36) Rohatgi, P. K.; Ray, S.; Liu, Y. *Int. Mater. Rev.* **1992**, *37*, 129.

Table 1. Hardness and Friction Data for Several Bearing Metals with a Nanosized Solid Lubricant Metal Filler

material	preparation method	Vickers hardness	coefficient of friction (steel counterbody)	ref
Al−Sn−Pb (nanocrystalline)	ECAP[a]	80−100		3
Al−Pb (60−220 nm Pb in Al)	MA[b]		0.4−0.5	8
Al−Sn (40−100 nm Sn in Al)	MA[b]	110	0.8−1.1	1
Al−Pb (nanosized Pb in Al)	rapid solidification	26	0.2−0.3	7
Co−Bi (present study (26 Bi))		**150**	**0.2**	

[a] Equal-channel angular pressing (severe plastic deformation). [b] Mechanical alloying (milling).

useful, but soft lubricant.[36] Comparison between sintering temperatures of 700 and 900 °C revealed no noticeable differences. This observation is rather unexpected given the changes in microstructures when using different sintering temperatures (Supporting Information Figure S9).

The highest Vickers hardness $HV_{0.1}$ of around 350 was measured for the lowest bismuth content (0.5 Bi, Figure 4b) and matches well with earlier values for pure cobalt of similar size and preparation method.[16] The high hardness values of the present metal/metal cobalt-based nanocomposites are considerably higher than conventional bulk (pure) cobalt.[16] The addition of small amounts of Bi causes a significant drop in the hardness and indicates changes in the material. However, compared to bulk hcp cobalt, the hardness is still superior. A similar hardness improvement was earlier explained by Grass et al. through nanovoids, a high content of crystal twins and the significantly reduced grain size.[37] Scanning electron micrographs (Figure 5) show fracture surfaces of nanocomposite 0.5 Bi sintered at 700 (a) and 900 °C (b) and confirmed the presence of nanovoids (arrows in part a) and significant twin formation (arrows in part b).

It is noticeable that high Bi content samples combine the hardness of bulk cobalt[35] and the friction coefficient of graphite[33] through addition of a very soft metal (Bi). This concept in principle follows the preparation of classical Babbitt metals but incorporates high hardness through structuring the hard constituent in the submicrometer scale. Table 1 compares the present material to earlier studies using severe plastic deformation or mechanical alloying for nanocomposite preparation.

In their present form, the nanocomposites shown here display an unacceptable high brittleness. It is assumed that the brittleness of the material is caused by the earlier identified bismuth oxide which appears to be located at cobalt grain boundaries (arrows in Supporting Information Figure S8). Improved sintering protocols and handling of all materials inside a closed system (glovebox and protective gas atmosphere) may allow circumventing oxide formation and result in less brittle composites.

(37) Hall, E. O. *Proc. Phys. Soc. London* **1951**, *64*, 747.

Conclusion

We have demonstrated a bottom-up route to metal/metal nanocomposites for the combination of material properties of immiscible metals. Cobalt and bismuth were chosen as model materials due to their thermodynamic immiscibility and their large difference in specific density, hardness, and melting point. The resulting cobalt/bismuth nanocomposites exhibited high hardness (the property of cobalt) and a low coefficient of friction (a property of soft materials such as graphite). The combination of physical and (presumably also possible) chemical properties demonstrated here of presently incompatible metals is expected to yield a broad variety of novel materials.

Acknowledgment. We would like to acknowledge financial support by ETH Zurich and the Swiss National Science Foundation (SNF 200021-116123).

Supporting Information Available: Overview of reported metal/metal nanocomposites with two immiscible elements (Table ST1); composition of as-prepared nanopowders (Table ST2); oxygen mass gain of the nanopowders upon passivation with air (Figure S1); transmission electron micrograph of the passivated nanopowder 26 Bi, HAADF-STEM micrograph, and EDX elemental analysis (Figure S2); temperature profiles of the sintering process (Figure S3); pill surfaces after sintering at 900 °C (Figure S4); pill surface of compacted nanopowder 10 Bi (Figure S5); X-ray powder diffraction patterns of two passivated nanopowders containing different bismuth loadings (Figure S6); scanning electron micrograph showing a cross-sectional view of a pill fracture surface (0.5 Bi sintered at 700 °C, Figure S7); scanning electron micrograph showing a fracture surface of sample 26 Bi sintered at 700 °C (Figure S8); scanning electron micrographs of fracture surfaces of sintered pills (Figure S9). This material is available free of charge via the Internet at http://pubs.acs.org.